

# Comprehensive geochemical/hydrochemical and geo-thermometry analysis of Unai geothermal field, Gujarat, India

Manan Shah<sup>1</sup> · Anirbid Sircar<sup>1</sup> · Nahid Shaikh<sup>1</sup> · Karan Patel<sup>1</sup> · Darshan Sharma<sup>2</sup> · Dwijen Vaidya<sup>3</sup>

Received: 1 February 2018/Revised: 17 July 2018/Accepted: 31 July 2018/Published online: 7 August 2018  
© Science Press, Institute of Geochemistry, CAS and Springer-Verlag GmbH Germany, part of Springer Nature 2018

**Abstract** The knowledge of water temperature produced from a geothermal reservoir and its composition is of utmost importance in designing utilization strategies, the surface production facilities and in selecting the material to be used. Unai hot springs are located in the southern part of Gujarat, India with discharge temperatures varying from 51 to 56 °C. With the aim of developing Unai as a potential geothermal field and exploiting it in the future, geochemical and geothermometrical study was undertaken. The samples were collected from various Unai geothermal location and analysis of chemical composition of water obtained from different wells was done. The concentration of Silica, carbonate and ions like Na and Cl have been analyzed to delineate the path of water movement in the subsurface and classify the reservoir based on the enthalpy.

The ratio of the concentration of ions like Na<sup>+</sup> and K<sup>+</sup> and the relative proportions of various sets of ions were also used to characterize the geothermal reservoir and the reservoir fluid by the use of ternary diagrams. Na–K–Ca, Chalcedony, quartz, and Silica geo-thermometers have been studied. The present study also envisages the importance of graphical representations like Piper diagram, Scholler etc. to determine variation in hydrochemical facies and to understand the evolution of hydrochemical processes in the Unai geothermal field respectively. The study yields the conclusion that the reservoir under consideration is a low enthalpy reservoir with temperature ranging from 60 to 80 °C.

**Keywords** Geothermal energy · Hydrochemical · Geochemical · Geothermometry · Renewable energy

---

✉ Manan Shah  
manan.shah@spt.pdpu.ac.in

Anirbid Sircar  
anirbid.sircar@spt.pdpu.ac.in

Nahid Shaikh  
nahid.sbt15@spt.pdpu.ac.in

Karan Patel  
karan.pbt15@spt.pdpu.ac.in

Darshan Sharma  
darshan.sharma@wipro.com

Dwijen Vaidya  
dwijen.vaidya@spt.pdpu.ac.in

<sup>1</sup> School of Petroleum Technology, Pandit Deendayal Petroleum University, Gandhinagar, Gujarat, India

<sup>2</sup> Wipro Limited, Bangalore, Karnataka, India

<sup>3</sup> Centre of Excellence for Geothermal Energy, Pandit Deendayal Petroleum University, Gandhinagar, Gujarat, India

## 1 Introduction

Numerous geothermal hotspots are found to be scattered over the entire stretch of Gujarat and the density of geothermal hot springs is found to be higher in the Saurashtra and Central region of Gujarat (Fig. 1b). Figure 1a demonstrates various thermal springs located in Gujarat, India.

Subsequent to the breakup of the supercontinent Gondwanaland, the Indian plate moved at very high speed (around 18–20 cm/yr during the Late Cretaceous period) and collided with the Eurasian plate giving rise to the Himalayas 50 Ma ago (Kumar et al. 2007). Currently, it is moving North-East at a speed of 5 cm/yr while the Eurasian plate is moving North at only 2 cm/yr. This is causing the Eurasian Plate to deform, and the Indian Plate to compress at a rate of 4 mm (0.16 in) per year. (GSI

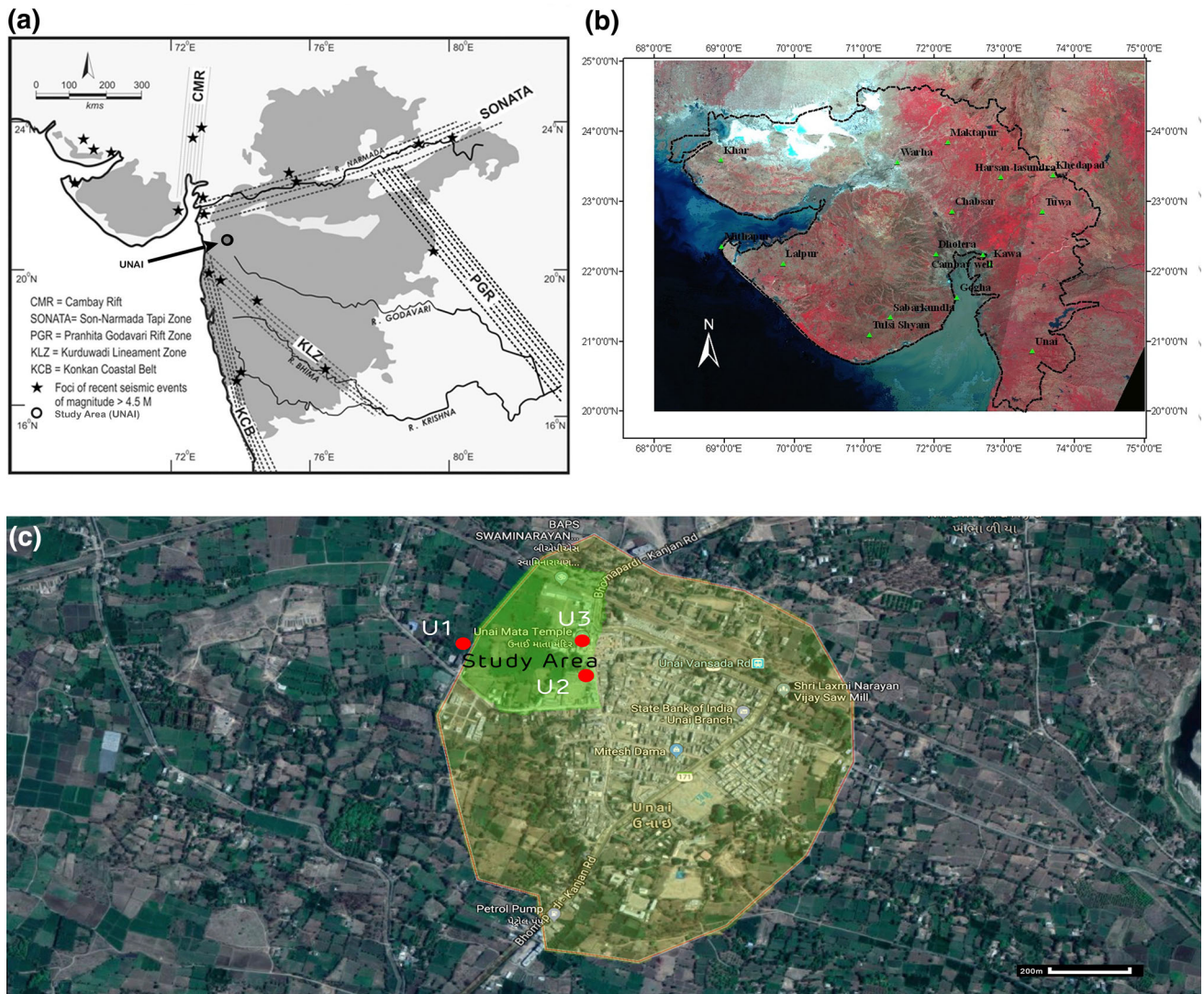


**Fig. 1** **a** Deccan Plateau uplift: insights from parts of Western Uplands, Maharashtra, India: Vivek S. Kale, Gauri Dole, Devdutt Upasani and Shilpa Patil Pillai; **b** location of various thermal springs in Gujarat, India. (Merh 1995); **c** Google map of study area and locations of wells

1991) Compressive intra-continental stress built up this way give rise to faults perpendicular to the direction of compression. Son-Narmada-Tapi fault zone running East–West through Central India is an example of the same (Kothyari and Rastogi 2013). Unai, chosen as the study area for this paper, lies in this zone. Thus, Son-Narmada-Tapi major fault zone ergo is accountable for the geothermal hotspot around Unai. This fact may prove to be useful while undertaking geothermal exploration, planning geothermal wells and in determining the direction of maximum reservoir permeability. Thus, drainage strategy maybe planned accordingly Fig. 1a portrays the geothermal provinces associated with Cambay rift and Son-Narmada-Tapi Fault Zone.

Singh et al. (2018) carried out geochemical and temperature studies for Tulsishyam hot springs located in

Gujarat, India which is located in the geographical vicinity of Unai hot spring. The temperature there is found to vary between 39 to 42 °C. This paper describes a similar attempt at predicting insitu conditions and propose a hydrodynamic model by geochemical and geothermometric study undertaken at Unai hot spring.

Unai is a developing area. As it develops, the electricity demand and arrangement for space heating and cooling facility become increasingly necessary. Exploitation of the underlying geothermal energy resource can be carried out using Organic Rankine Cycle to generate electric power and Ground Source Heat Pump can be used for cooling and heating of domestic and commercial buildings. The planning of exploitation strategies of the geothermal water obtained from Unai necessitates obtaining the knowledge of the expected temperature ranges of the reservoir and the

composition of the produced fluid. Thus a study to determine reservoir temperature was undertaken based on ionic and silica geo-thermometry. Three water samples were collected from different geothermal hot springs at Unai and were analyzed for the parameters concerning the physico-chemical parameters like pH and the dissolved chemical species (major, minor, trace elements and ions) like silica,  $\text{Na}^+$ ,  $\text{Ca}^{+2}$ ,  $\text{K}^+$ ,  $\text{Cl}^-$ , etc. were measured and analyzed. The variation in the chemistry of geothermal fluid data gives some input on the following characteristics of a deep geothermal reservoir: reservoir temperature (or reservoir depth if the geothermal gradient is already known), type of reservoir rock, mixing processes, multiple fluid origin, elevation of the infiltration basin, underground transit time, behavior of fluid exploitation. It also helps in quantifying the processes that govern their compositions and the associated chemical and mineralogical transformation of the rocks with which the fluids interact and helps in building a conceptual model. The samples have been collected with absolute care to maintain the representativeness of the samples and also while testing to provide reliable results. The study was done by collecting samples, analyzing their chemistry and interpreting the composition in terms of geology and subsurface temperature.

## 2 Study area

There are 22 thermal provinces in Gujarat having 17 thermal spring that stretch from Archean to Quaternary in provenance within the Cambay basin as its main tectonic structure. The geothermal field at Unai is located in southern part of Gujarat (Fig. 1a). This place is located 100 km from the Cambay Basin, which hosts prominent oil and gas fields (Fig. 1b). The elevation of the surrounding area ranges from 10 to 55 m. The area is mostly surrounded by dense forest and small hillocks. The terrain is largely covered with the thick Deccan trap of Late Cretaceous to Early Eocene age (Biswas 1987). The reason for conducting the study at Unai is that the area has registered high heat flow and has hot water spring at Unai Mata Temple (Vaidya et al., 2015) (Fig. 1c).

## 3 Geology of study area

The geological developments in the southern part of Gujarat range from Cretaceous to Holocene and nowhere older rocks are accounted to occur whether on-surface or in sub-surface. Geologically, South Gujarat has evolved with the breakup of the Gondwanaland. Sedimentation and volcanism initiated, during early Cretaceous with the marine transgression along the Narmada geofracture gave

rise to the equivalents of Bagh beds. Subsequent events comprised Deccan volcanism and development of the Cambay basin (Cambay and Narmada-Tapi grabens) which became the site of the Tertiary sediment accumulation. Quaternary deposits are equally well-developed and mostly comprise of alluvial accumulations and coastal marine deposits (Sircar et al. 2015; Shah et al. 2018a, b).

The Unai hot spring is located in Narmada-Son Lineament. A mid-continental rift system called Narmada-Son Lineament (NSL) (Fig. 2), divides the Indian shield into two halves (Mehr 1995). One half is a thick pile of Deccan lava flows which predominated in the western part of NSL. The basaltic lava flows of the Deccan Trap constitute the major rock formation of the southern part of Gujarat. These trappean rocks comprise of horizontal lava flows and covers a large portion of the area. They are compound flows and each flow unit consists of different subflows. Due to variation in the hardness of the different flows, and of parts of the flows, the trap shows flat-topped hills. The traps attain their maximum elevation near the border of Gujarat and Maharashtra, i.e. Dangs area, where they show escarpments of about 1200 m height (Biswas 1999; Rao and Tewari 2005; Rao et al. 2012; Tewari et al. 2009).

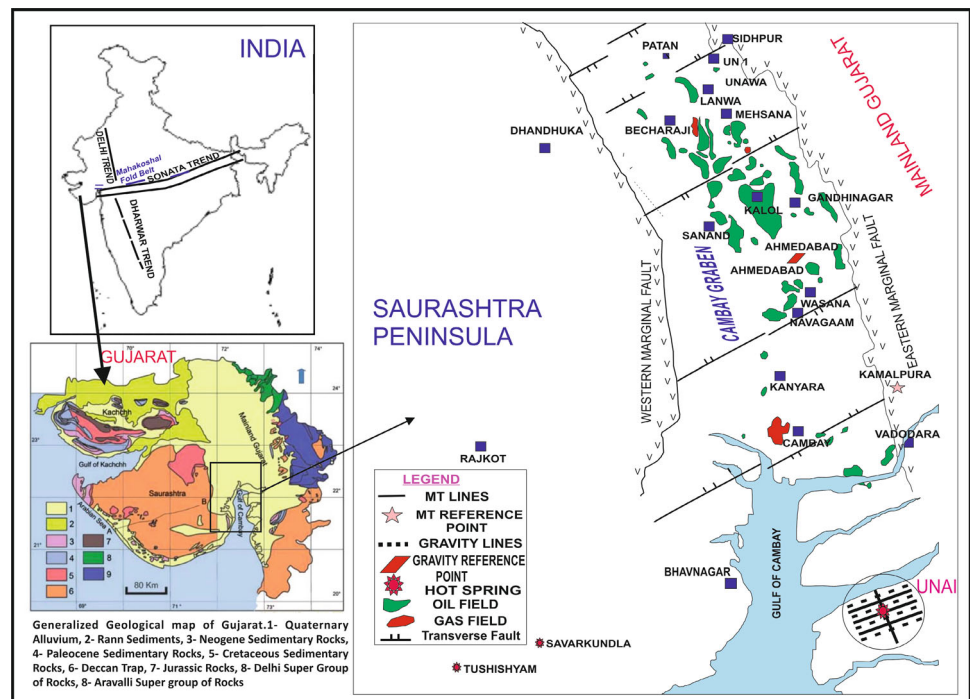
Lava-flows comprise dark grey basalts of several varieties, quite often amygdaloidal and/or porphyritic. The trappean rocks are highly jointed showing several sets, mainly ENE-WSW to E–W and NNE-SSW to N–S directions. Also, there may be a possibility of hard rock present beneath the subsurface. This hard rock shows NE-SW trend of foliation with the dip towards NW (Anand and Rajaram. 2004). The hot spring at Unai located along N-S trending regional fault and it is in the western part of NSL. The thermal manifestation is in the form of hot spots, which show profuse discharge of hot water with small amount of gas emission (Singh et al., 2015).

## 4 Sampling method and analysis techniques

Representative water samples from the drilled wells were collected for the laboratory analysis. The sampling methods used are as outlined in (Giggenbach and Goguel, 1989). There were three samples collected from each water source:

Samples from all the three wells were collected after pumping out for 15 min to prevent non representative sample and polluted water. The parameter such as temperature, electric conductivity (EC) and pH were measured in the field immediately after sampling using a multiparameter WP600 series meter. Preservation of samples was critical in order to reduce the rate of any biological or chemical reactions. The bottles were rinsed using groundwater to be sampled and were stored in the acid washed

**Fig. 2** Geological map and tectonic framework of Gujarat. This figure also gives the detailed fault distribution system, MT profiles, gravity lines, hot springs, oil and gas field locations in the area (Sircar et al. 2015)



Ploythylene bottles. Also, the samples were filtered on site using an acetate cellulose filter paper having pore size of 0.45  $\mu\text{m}$ . After collecting the samples, these were evaluated in our laboratory where all the chemical tests were carried out in order to obtain concentration values (Shah et al. 2015). Standard APHA methods were used to determine the concentration of Chloride, Sulphate, Fluoride, Calcium, Magnesium,  $\text{HCO}_3^-$ , Boron, Arsenic, Iron, Magnesium, Silica, Lead and Nickle (APHA 2012). Inductively coupled plasma mass spectroscopy (ICP-MS) has been used for the analysis of Strontium, Caesium, Rubidium and Barium. To determine the Sodium and Potassium content Flame photometric and EDTA method was used (Armijo 2012).

Calculation of subsurface temperature is an important application of surface-water geochemical analysis. Geothermometry is an exploration technique which can help us to predict the temperature of the geothermal system and monitor temperature change in the reservoir during production (Powell and Cumming 2010; Wishart 2015). Geothermometry can also help to understand the chemical state of recharging water as a result of the effect of temperature and pressure (Bruhn et al. 2011).

In this study solute geo-thermometers such as silica and cations were used to estimate the temperature of the geothermal reservoir.

The Na–K indicator by Fournier (1979), Na–K indicator by Nieva and Nieva (1987), K/Mg indicator by Giggenbach (1986), Quartz conductive by Fournier and Potter (1982) and Quartz adiabatic by Fournier (1977), are few of the

most well-grounded geo-indicators used to predict reservoir characteristics.

Reservoir temperature was estimated by employing the Na–K–Ca or Na–K–Ca (Mg corrected) geothermometric method, the resultant temperatures were found to be either too elevated or too depressed than the actual subsurface temperature and thus were rendered to be unreliable.

Wishart (2015), pointed out that the causes for exaggeration of temperature by these geo-indicators may be due to either: equilibration at conditions that have higher temperatures and are seated deeper than the existing areas of mixing and circulation of groundwater, or heat dissipation due to conduction. The water-dissolving property of silica at high temperature has proved to be of great use as a geothermal indicator (Truesdell and Hulston 1980; Fournier and Potter 1982). Equilibration is affected by quartz at about 180–190  $^{\circ}\text{C}$ . On the other hand, Chalcedony controls equilibration at a comparatively lower temperature (Arnorsson 1976). Quartz adiabatic and Quartz conductive are two silica-based geo-indicators that are stable at lower temperature (Truesdell and Hulston 1980).

Wishart (2015), also described that the silica geo-thermometry might underestimate the temperature than the actual predominating conditions in the reservoir due to:

- I. Change in solubility caused by the presence of highly saline fluid. For example, the water may contain high concentrations of  $\text{Na}^+$ ,  $\text{K}^+$ , and  $\text{Cl}^-$  ions.
- II. Precipitated silica due to loss of steam

III. Modification in the pH due to mixing with cold meteoric water which has influenced quartz stability and dilution.

Hence, the cation geo-thermometry proves to be more authentic. Numerous plots were analyzed based on the chemical composition, Tcsh, Tc1b, Durov and Piper-naming a few and it was concluded that the water is of alkaline type of the under mature water category region and that the water has been mixed with water of lower temperature as well as concentration. In such case, cation geo-thermometry such as Na/K or Na/K/Ca were found to be more genuine as compared to the others (Wishart 2015; Giggenbach 1991b). Moreover, Wishart (2015), also stated that re-equilibration of Na/K geothermometer is slower than that of quartz geothermometer and is less affected by dilution. But owing to the considerations taken for application of suitable geothermometry, silica geothermometry fits best for the study area. As such experimentally derived equations describing quartz solubility (silica geothermometry) are good between 0 and 250 °C accurate to about  $\pm 2$  °C. Whereas, the basis of cation geothermometer is equilibration between water and rocks and it works best for fluids derived from a thermal environment  $> 180$  °C. Even though precipitation of silica, silica solubility, effect of pH and dilution may under estimate or over estimate the temperature of reservoir estimated from Silica geothermometry but it is well sufficing the condition of temperature estimation on basis of silica dissolution rather than equilibration. As temperature of the reservoir is not known or measured using any downhole temperature measurements, application of cation geothermometry considering the reservoir temperature above 180 °C attaining the equilibration will be the estimation with no basis.

## 5 Results and discussions

### 5.1 Water quality characterization

#### 5.1.1 Hydrochemical characteristics

The water samples from the hot spring of Unai indicates that the pH values range is 7.5–8.5 (Table 1), which indicate that the spring water is moderately alkaline in nature. The temperature values ranged from 51 to 56 °C in the study area. The temperature of discharging thermal water does not show any significant variation, and the temperature varies within a range of 1 to 5 °C for all three thermal springs. The  $\text{SO}_4^{2-}$  values of the water samples ranged from moderate to high (41–108 mg/L). This suggests mixing of volcanic gases with the thermal waters (Singh et al. 2014; Zimik et al. 2017). Chloride content in Unai hot

**Table 1** Results of analysis of water samples

Parameters	Unai 1 U1	Unai 2 U2	Unai 3 U3
Surface temperature (°C)	51.3	55	56
pH	8.38	7.86	8.12
TDS	998	1190	1114
Chlorides (mg/l)	345	525	530
Sulphates (mg/l)	41.17	108.8	92.65
Fluoride (mg/l)	2.3	8	8.4
Conductivity (Ms/cm)	1475	1840	1662
Sodium (mg/l)	158	324	340
Potassium (mg/l)	13	15	10
Calcium (mg/l)	168.34	52	64
Magnesium (mg/l)	5	17	4.86
Carbonate (mg/l)	4.8	–	4
Bicarbonate (mg/l)	126	42	42
Boron (mg/l)	–	–	–
Silica (mg/l)	21.05	32.26	32.16
Lead (mg/l)	0.15	0.22	–
Nickel (mg/l)	–	0.09	0.07
Salinity	623	948	957
Carbonate hardness	260	84	96

springs ranged from 350 to 550 ppm. Presence of chloride content determines the dilutions or contribution of deep thermal water. Hot spring with significant chloride content is consistent with the outflow of a geothermal reservoir. High chloride content may harm metallic pipes and structure, as well as growing plants. Thermal water from Unai contains high Na ranging from 158 to 340 mg/L. It indicates that water circulating in deep and it may be a high-enthalpy geothermal reservoir (Powell and Cumming 2010). Sodium and chloride are the dominant species present in the hot spring water discharging from Unai geothermal field. Calcium, Magnesium and Potassium are present in much lesser concentrations. The concentration of  $\text{HCO}_3^-$  ranges between 42 and 126 mg/L. Higher  $\text{HCO}_3^-$  concentrations have been observed specifically in those locations where lower Cl concentrations has been registered (Zimik et al. 2017) Unai water samples have salinity values which ranged from 623 to 957 mg/L indicating the water is low to moderate saline. The conductivity values are moderate in nature. It indicates a bulk change in total concentrations of dissolved cations and anions. High amounts of dissolved minerals and salt concentration in water yield high conductivities. The EC of water is an indirect measure of the total dissolved solids (TDS) content of water, and there is usually an approximately linear relationship between TDS and conductivity. The water

samples show a low level of carbonate. The low level of carbonate and bicarbonate components is an indication that the water has risen up from deeper levels influenced by the formation water chemistry from the deeper sedimentary layer under the trappean flows (Nicholson 1993; Sharma 2013). This may also indicate that the Fluorine content ranged from 2 to 8 mg/L which is higher than acceptable drinking water guidelines indicating the water is in interaction with subsurface mica and apatite bearing rocks (WHO 2004). The water samples showed that silicon values were between 21 and 32 mg/L. Such silicon contribution is expected in deep waters with a high thermal gradient. Silicon gets dissolved from alkali feldspar, quartz and amorphous silica (Sharma 2013). The presence of zeolite in the rocks of study area suggests that the water has interacted with the basement rocks and then migrated to the shallow level. It can be said that tectonic movement and mantle upliftment might have created higher flow gradients which in turn heat the water, which rises back to the surface as it reaches its boiling temperature. (Sircar et al. 2015)

## 5.2 Hydrochemical facies

Graphical representation of groundwater major dissolved constituents helps in understanding its hydrochemical evolution, grouping and areal distribution (Shah et al. 2018a, b).

Water samples have been analyzed by the interpretation of various analytic plots of water classification and geo-indicator plots to estimate variation in hydrochemical facies. The significance of the plots has been summarized in Table 2.

### 5.2.1 Piper plot

The Hydrochemical evolution of spring water can be understood by plotting the major cations and anions in the

Piper tri-linear diagram and Durov diagram. Piper (1994) explained the classifications the type of water facies on the basis of its interaction with rock and soil minerals. It has two separate trilinear plots of cations and anions respectively relative concentration of each other. The diamond plot at the center is blended of two trilinear plots on the two sides of the diamond. Different quadrants of diamond show the different type of water on the basis of dominance in ion concentration as shown in Fig. 3. Figure 3 illustrates the representation of the obtained results on the piper diagram. From the analysis of samples of water from Unai, it was found that U2 and U3 fall in Sodium Chloride water region while U1 was in Calcium Sulphate dominated water region. The change in ionic composition of samples might be result of two different water source, temperature dependent dissolution/precipitation of ions in their flow path, mixing of surface water with underground aquifer or contamination by saline water or cement pollution (as water is found rich in Calcium Sulphate) (Todd 1980; Sakram et al. 2013).

### 5.2.2 Durov plot

Durov (1948) plot is advantageous in revealing the geochemical process that can alter the groundwater quality (Lloyd and Heathcoat, 1985). There are two trilinear plots of cations and anions respectively. Point of intersection of lines from trilinear diagrams of the same water sample in the binary plot will define the hydrochemical process (like dissolution or precipitation) involved along with the type of water (i.e. rich in NaCl or CaCO<sub>3</sub>, etc.). Here, U1 has a relatively higher concentration of Ca and HCO<sub>3</sub><sup>−</sup> + CO<sub>3</sub><sup>2−</sup> and lower concentration of NaCl as compared to that of U2 and U 3 (Fig. 4a). So the temperature of U2 and U3 might be higher than U1. This is because on increasing temperature, CO<sub>2</sub> is liberated and so CaCO<sub>3</sub> gets precipitated. This results in lesser Ca<sup>2+</sup> and CO<sub>3</sub><sup>2−</sup>/HCO<sub>3</sub><sup>−</sup> concentration in U2 and U3, moreover with increasing

**Table 2** Significance of plots

Types of plots	Significance
TCSH	Illustrates the proportions of the major anions present in geothermal water which can further helps to classify the geothermal system or different types of geothermal system
TCFB	This ternary of chloride, fluoride and boron is useful in tracing sources of water
TCLB	The ternary of chloride, lithium and boron is used to distinguish fluids from different sources, to reveal fractionation associated with boiling or mixing with fluids that have boiled, or fluids generated by different sources of high temperature steam
Schoeller	Pictorial representation for relative abundance of major cations and anions
Durov	Durov plot defines Hydro-chemical processes involved along with water type
Piper	It is used to classify the samples on basis of different types of water like Sodium chloride water, Calcium Sulphate water, Sodium bicarbonate water and calcium bicarbonate water

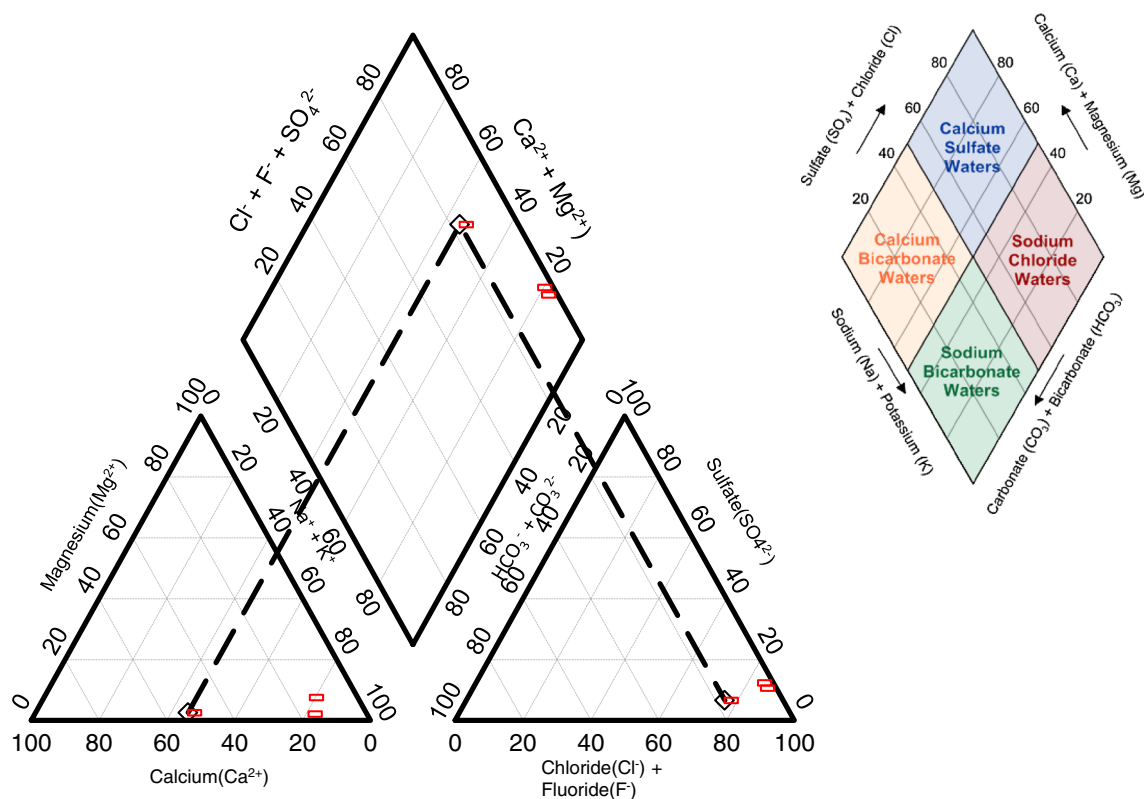


**Fig. 3** Piper trilinear diagram showing hydrogeochemical facies of water samples of studied area

temperature, dissolution of NaCl increases. Higher Na<sup>+</sup> and Cl<sup>-</sup> in U2 and U3 as shown by Piper Plot, and Durov Plot also indicate the higher temperature as compared to U1. Thus the temperature of U2 and U3 might be higher than that of U1. But there are many more factors playing role in altering geochemistry of groundwater, so various other plots and graphs should be integrated to get the conclusion.

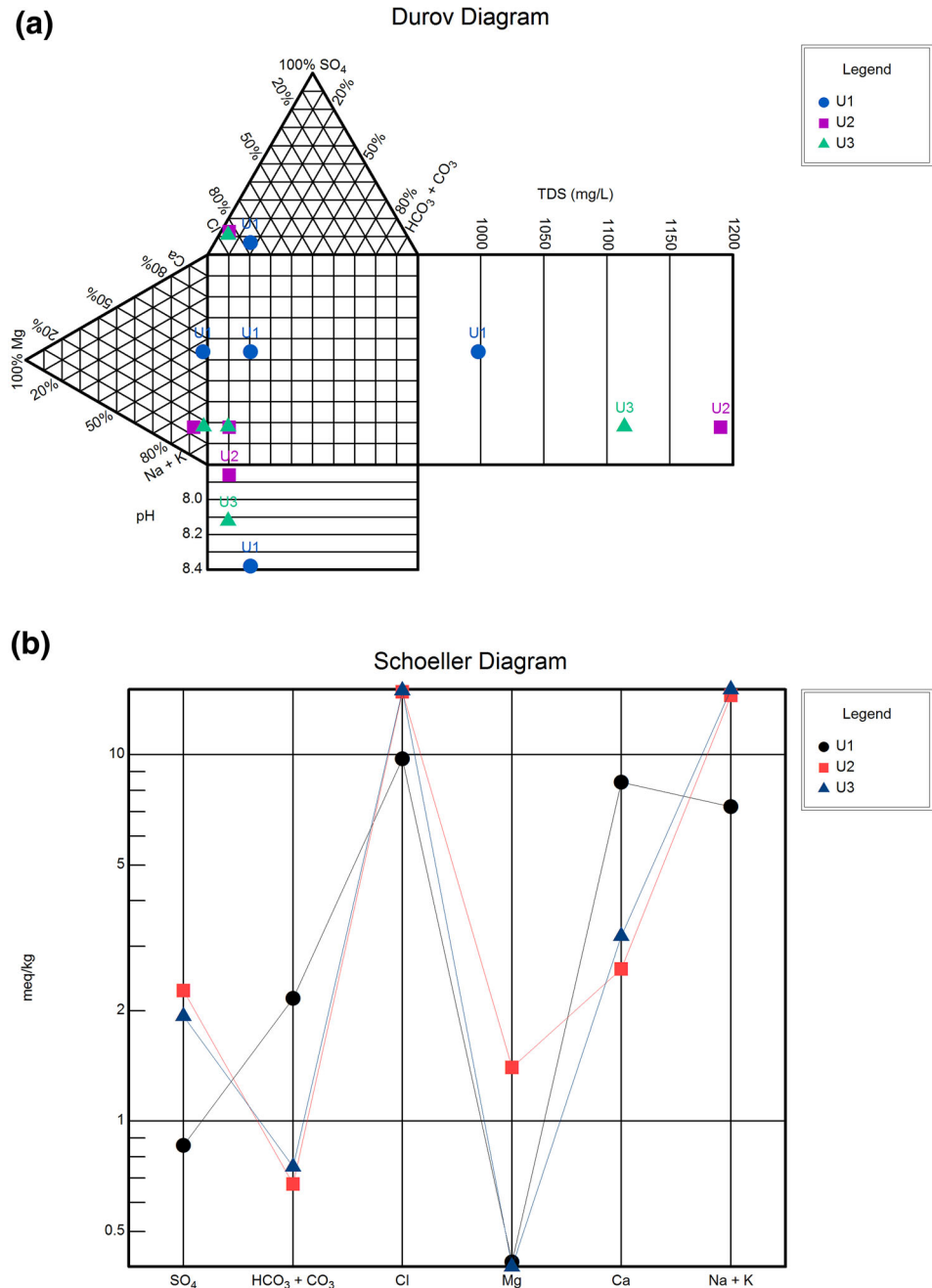
### 5.2.3 Schoeller plot

Schoeller (1961) proposed a semi-logarithmic graph in which major anions and cations are plotted on the horizontal axis with six equal divisions and the vertical scale is the logarithmic scale of an equivalent concentration of these ions. Points then are connected by polyline and slope of the line between two ions can be compared with other samples to visualize the correlation between two ions. The plot shows great compatibility between U2 and U3 (Fig. 4b). Though U1 is differing from other two, all the samples are dominated by Na + K in cations and Cl in anions.

### 5.2.4 TCSH plot

The TCSH plot (Giggenbach and Gougel 1989; Giggenbach 1991a) illustrates the proportion of major anions present in the sample, Cl-SO<sub>4</sub>-HCO<sub>3</sub> ternary diagram is primarily used to classify the types of geothermal water of a field under investigation (Fig. 5a). Volcanic water, steam heated water, peripheral waters and mature matters are the different types of geothermal water that can be distinguished from the ternary diagram. Chemical data from Table 1 is plotted in the Cl-SO<sub>4</sub>-HCO<sub>3</sub> ternary diagram. U1, U2, U3 falls on the Cl rich domain of geothermal water which is mature water and is close to the Cl apex. U2 and U3 fall near to the Cl-SO<sub>4</sub> indicating appreciable sulfur content. The dominance of SO<sub>4</sub> over HCO<sub>3</sub> in U2 and U3 as compared to that of U1 suggests that the thermal water might have been mixed with marginal steam heated water or during the water-rock interaction, interacting with the sulfur-bearing environment. High Cl concentrations indicate that waters fed directly from the deep reservoir with minimal mixing or conductive cooling. Water enriched in Cl may be an indication of the influence by seawater intermixing with thermal fluids. Relative to the abundance of chloride, sulfate and bicarbonate concentrations in the geothermal water, the Cl-SO<sub>4</sub>-HCO<sub>3</sub> ternary diagram showed the water is alkali chloride type with relatively low

**Fig. 4 a** Durov plot depicting hydrochemical process involved (Lloyd and Heathcoat 1985); **b** Schollers plot



sulfate and bicarbonate concentrations (Rybach and Muffler 1981).

### 5.2.5 TCLB plot

The ternary plot of Chloride, Lithium, and Boron that first presented in Giggenbach (1991a) was used to distinguish fluids from different sources, to reveal fractionation associated with boiling or mixing with fluids that have boiled or fluids generated by different sources of steam.

Boron, chloride, and Lithium are tracers for fluid from geothermal waters. Boron may be leached from wall rocks and Lithium indicates the migration of thermal fluids from deeper geothermal sources. U1, U2, and U3 all plot in the absorption of low B/Cl steam region of the Cl–Li–B ternary diagram suggesting that this water emerges from aging hydrothermal system (Fig. 5b) (Urzueta et al. 2002; Powell and Cumming 2010).



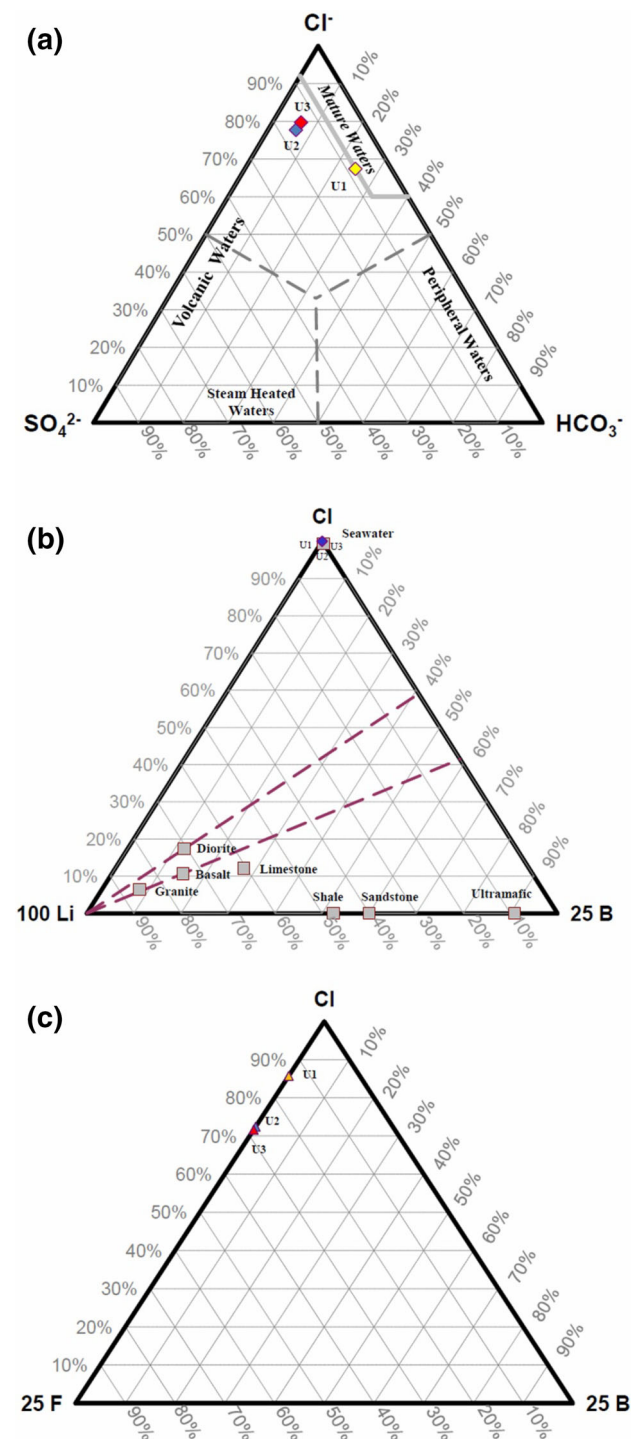


**Fig. 5** **a** Cl-SO<sub>4</sub>-HCO<sub>3</sub> (TCSH) ternary anion plot (Giggenbach and Goguel (1989)); **b** Cl-Li-B (TCLB) ternary plot (Giggenbach 1991a, b); **c** Cl-F-B (TCFB) ternary plot (Giggenbach 1991a, b)

### 5.2.6 TCFB plot

The ternary plot of Chloride, Fluoride, and Boron is useful in tracing sources of water. Fluoride can be expected to be conservative. U1, U2 and U3 all fall on the Cl-F line as

there is no trace of boron in the three samples (Fig. 5c). Traces of fluorine indicate soluble group species. They pass into the solution often before appreciable alteration of the host rock has occurred. Fluoride content is 2–9 mg/L which exceeds the acceptable drinking water indicating that the water is in interaction with subsurface mica and apatite bearing rocks (Powell and Cumming 2010).

## 5.3 Geothermometry

The cation geothermometers indicate temperatures higher than the quartz geothermometer as shown in Table 3. Lower temperature estimation by silica geothermometry could either be due to deposition of silica during ascent of the fluid to the surface or mixing with colder fluid. Mixing does not affect the cation geothermometers as much as the quartz geothermometer. Various plots were used to understand the maturity of water samples in terms of equilibration attained with the particular cations and hence thereby temperature prediction from the plots.

### 5.3.1 TNKM plot

Na–K–Mg ternary diagram was proposed by Giggenbach (1988). It is the most widely used cation geo-thermometry plot, a ternary plot combining the sodium–potassium (Na–K) geo-thermometers with the potassium–magnesium (K–Mg) geo-thermometer. This ternary diagram is used to determine the reservoir temperature and to recognize waters which have attained equilibrium with host lithologies. U1, U2, and U3 all fall near to the Mg vertex indicating that the waters are partially equilibrated or mixed. U1 and U2 lie below the immature water curve indicating an initial dissolution of minerals before equilibrium sets in. Water from well U3 lies in the partial equilibrated region suggesting that dissolution of minerals has taken place or, the equilibrium reactions have set in but equilibrium has not been reached or the collected sample is a mixture of a water that has reached equilibrium with a diluted unequilibrated water such as cold groundwater. U1 and U2 are immature water suggesting that geo-thermometry cannot be applied to this water. Study of sample from U3 gives a temperature of 60–80 °C indicating that the field may qualify to be a low temperature geothermal system (Fig. 6a).

### 5.3.2 XKMC plot

Giggenbach and Goguel (1989) refer to this cross-plot as a “geoinicator” rather than a geo-thermometers plot because it compares the potassium-magnesium geo-thermometers with a measure of the partial pressure of CO<sub>2</sub> - based upon the equilibrium between K-feldspar, calcite,

**Table 3** Temperature obtained from geochemical analysis results

		U1	U2	U3
Geothermometry				
Silica geothermometry				
Quartz	Fournier and Potter (1982)	65.64207	82.938283	82.80794
	Fournier (1977)	65.37737	82.427467	82.29728
	Arnórsson et al. (1983)	50.56542	68.145373	68.01183
Chalcedony	Fournier (1977)	33.37726	51.24205	51.10463
	Arnórsson et al. (1983)	36.88015	53.780394	53.65085
Cation geothermometry				
Na–K	Arnórsson et al. (1983)	175.9013	127.71726	96.43122
	Fournier (1979)	209.267	165.81134	136.6862
	Giggenbach (1988)	217.1993	177.49706	150.4395
Na–K–Ca	Fournier and Truesdell (1973)	151.4024	144.84138	124.1627

and K-mica on one side and the dissolved  $\text{Ca}^{+2}$  and  $\text{K}^{+}$  on the other. The cross-plot helps to determine the partial pressure of  $\text{CO}_2$  at the last temperature of the water equilibration with rock, as determined by the K–Mg geothermometers. Samples here are located above the saturation line hence partial pressure of  $\text{CO}_2$  is less than the required to drive the reaction of dissolution of Calcium–Aluminium Silicates to Calcite. Hence chemistry of the water at sample depth is not governed by rock dissolution. Moreover, evaluation of Partial Pressure of  $\text{CO}_2$  on basis of K–Mg geothermometry is reliable for water enriched with  $\text{CO}_2$  or bicarbonates. However, from the given plot, it can be observed that temperature of U1 ( $\sim 80^\circ\text{C}$ ) is found highest among all ranging from 70 to  $80^\circ\text{C}$  (Fig. 6b) (Powell and Cumming 2010; Shah et al. 2017).

### 5.3.3 XMCKN plot

The temperature of geothermal fluids can be estimated from relative concentrations of cations like Na–K–Ca–Mg. Cation geo-thermometers are based on the assumption that the concentrations depict the last equilibrium state of fluid and rock interaction. From the relative concentrations, the temperature of equilibrium state can be estimated and hence the temperature of the geothermal reservoir. As seen in the Fig. 6c, samples are scattered from equilibrium line, indicating the non-equilibrium state of rock and fluid interaction due to dissolution. Thus estimating temperature on basis of cation geo-thermometry might not be reliable as equilibration- which is the basis of cation geo-thermometry has not yet achieved (Giggenbach and Goguel 1989).

From the ternary plots, we may conclude that the geothermal water is from a low-enthalpy geothermal system. The results obtained from cation geo-thermometry can be ignored which indicate that the geothermal water from Unai belongs to a low enthalpy geothermal system with temperature ranging from 60 to  $80^\circ\text{C}$  (Fig. 6c). Wishart (2015) also

stated that the overestimation of temperature by geoinicator is due to equilibration conditions that are hotter and deeper than existing areas of mixing and circulation of groundwater.

### 5.3.4 XCIHquartz plot

Enthalpy-chloride diagrams are useful in understanding the hydrology of a geothermal field. It is a suitable tool to distinguish the effects of boiling and mixing. Enthalpy is based on quartz geo-thermometers temperature. Enthalpy is derived from the Fournier and Potter (1982) quartz geothermometers using a fourth order polynomial curve fit of the enthalpy of pure water between 80 and  $340^\circ\text{C}$ . U1, U2, and U3 lied along the mixing line (Fig. 7a). They are probably cooled by two processes, the ascending deep hot water boiled and then mixed with cold water at shallow depth. This demonstrates that water is a low enthalpy geothermal system.

### 5.3.5 XKMS plot

This cross plot of the K–Mg and quartz geo-thermometers is from Giggenbach and Gougel (1989). The plot uses the chalcedony geo-thermometers, which is regularly more precise to use than quartz for water from a lower temperature geothermal source (Love et al. 2014). Figure 6 is a plot of K–Mg and the quartz (conductive) geothermometers. U1, U2, and U3 samples gave geo-thermometers temperatures ranging from 65 to  $82^\circ\text{C}$ . U2 plots at a lower temperature at of  $65^\circ\text{C}$ , whereas U1 gives a geo-thermometers at a higher temperature of  $82^\circ\text{C}$  (Fig. 7b) (Lajwe 2013).

### 5.3.6 Conceptual hydrodynamic model

The current theoretical comprehension of hydrodynamics in aqueous systems might be communicated as (Fig. 8).

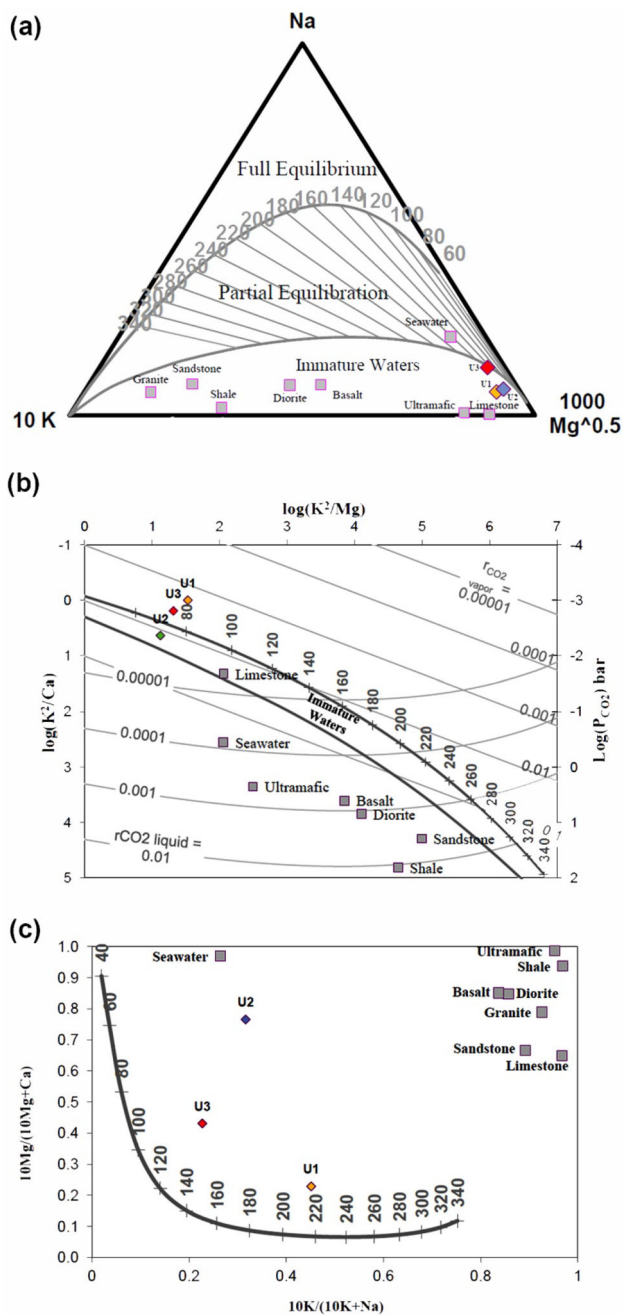


**Fig. 6** a Graphical evaluation of the water–rock equilibration temperatures (Giggenbach 1988) using relative Na, K, and Mg; b diagram showing Log (K<sup>2</sup>/Ca), Log (K<sup>2</sup>/Mg) and Evaluation of CO<sub>2</sub> partial pressures (Giggenbach 1988); c diagram showing 10 Mg/(10 Mg + Ca) versus 10 K/(10 K + Na) plots for the geothermal hot springs in (mg/kg). (Giggenbach and Goguel 1989)

This model has been developed based on the geochemical and surface temperature data. The following paragraph illustrates the conceptual fluid flow model postulated for the present study. One of the most important elements of a geothermal reservoir is the cap rock which prevents cold ground water from invading into the high temperature

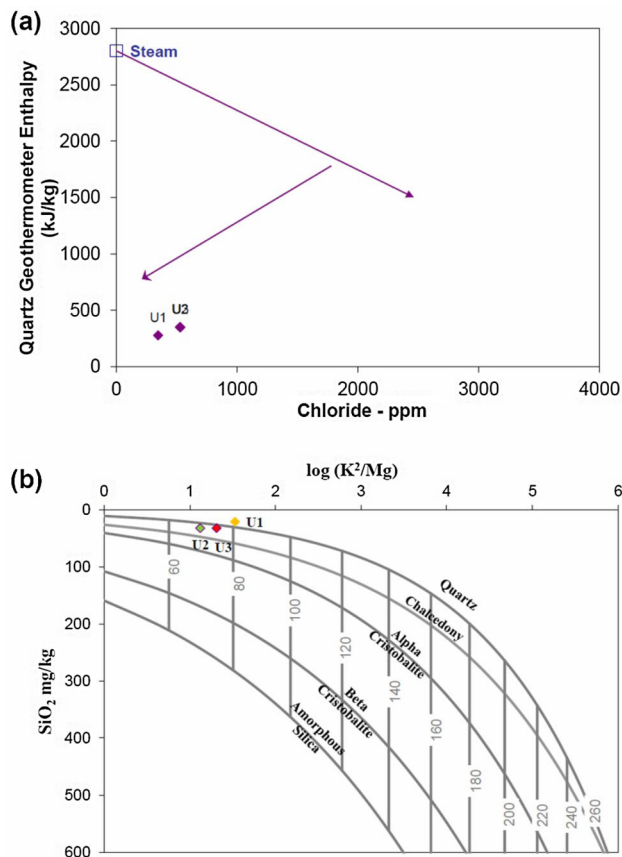
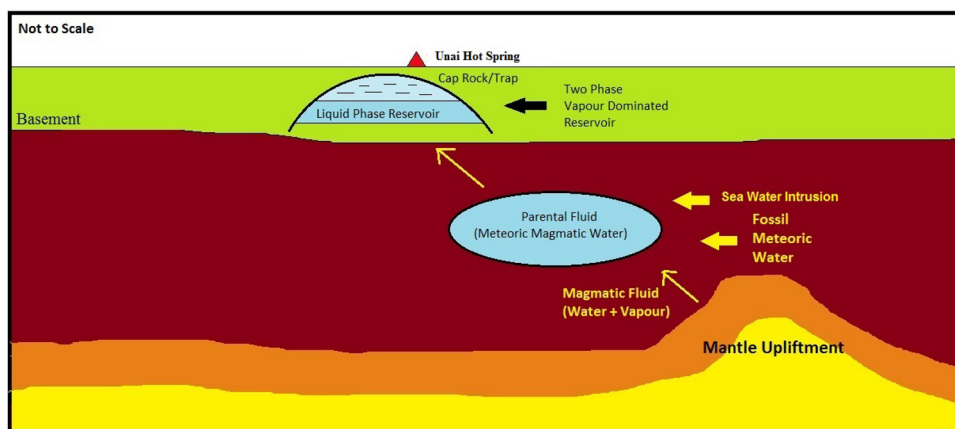


**Fig. 7** a Quartz geothermometry plot; b cross plot of K<sup>2</sup>/Mg versus Silica geothermometer results for hot springs (Giggenbach 1988)

reservoir. Figure 8 depicts that the parental fluid ascends through the high permeable zones developed along the faults which characterize this region. The high resistive rock exists at the deep sub-surface while the geothermal source exists in deep regions with manifestations at shallow depths due to circulation aided by convection cells. It postulate that both are connected through fault systems. Certain confidences in these models are provided by the results from the acquired MT survey results at the study area (Sahajpal et al. 2015). The main direction of movement at the central section of the acquired profiles appears to be vertical with very limited lateral movement. The faults identified are normal in nature. The ascending hot fluid yields convective circulation systems beneath the cap rock. The fluid reaching shallower part may be from a two phase or vapour dominated reservoir. Furthermore, meteoric water from the recharge area descends through sub-vertical channels, such as permeable faults or sub-vertical intrusive body contacts, to a deep heat exchange high-temperature zone. By penetrating meteoric waters to deeper zones, the geothermal system is fed and the fluid flow circle is eventually completed (Niarraq et al. 2017). The

**Fig. 8** Conceptual hydrodynamic model of Unai geothermal field



resulting mixing converts the meteoric water to high temperature NaCl enriched “parent geothermal fluid” through heat and chemical exchange. Basically, the “parent geothermal fluid” of geothermal systems has two components: meteoric water and magmatic fluid. Deep level magmatic fluid contributes contents like HCl, HF, SO<sub>2</sub>, H<sub>2</sub>O, H<sub>2</sub>S gases which convert to dominant NaCl form due to interaction with the host rocks in the subsurface. The fluids then ascend through high-permeable zones (“geothermal reservoirs”), and finally discharge at the earth surface in the form of hot springs. Flows from recharge to discharge areas are driven by pressure and fluid density differences (forced and free convection) (Kiriyukhin et al. 2003).

## 6 Conclusion

The study proves that the geothermal waters in this region are rich in ions such as Sodium, Potassium, Chloride, silica content and Sulphate. From the study of geothermal springs of Unai, various plots indicate low to moderate Na–Cl content. Water has not attained equilibrium in interaction with rocks, hence temperature prediction on basis of various geo-thermometers may not be that reliable. But reliable temperature prediction can be made by Silica geothermometry as it is based on dissolution of amorphous silica, chalcedony or quartz at the specific temperature range, rather than equilibration attained. Moreover, water might have gone through various dissolution–precipitation processes or contamination from other sources which leads to an inappropriate estimation of its chemistry and temperature of the geothermal reserve. Though water collected from shallow depth shows its potential as low enthalpy geothermal resource, for better prospects, drilling to greater depth and taking representative samples will help in clarifying the hydro-geochemistry characteristics of water along with more accurate temperature prediction. The

entire study suggests the existence of a mature geothermal system in the region. This encourages researchers for further investigation of geothermal energy of this field.

**Acknowledgements** The authors are grateful to Pandit Deendayal Petroleum University for the permission to publish this research. Authors are thankful to Mr. Gaurav Negi for his technical support. Authors also acknowledge the technical support provided by Maharaja Sayajirao University and Kadam Environmental Consultants Private Limited

### Compliance with ethical standards

**Conflict of interest** The authors declare that they have no competing interests.

**Availability of data and material** All relevant data and material are presented in the main paper.

**Consent for publication** Not applicable.

**Ethics approval and consent to participate** Not applicable.

## References

- Anand SP, Rajaram M (2004) Crustal structure of Narmada-Son lineament: an aeromagnetic perspective. *Earth Planets Space* 56:9–12
- APHA, Awwa, WEF (2012) Standard methods for examination of water and wastewater, 22nd edn. American Public Health Association, Washington
- Armijo CF (2012) Water journeys II. Granada’s spas and springs through travellers’ and hydrologists’ eyes. Solprint, Madrid
- Arnórsson B (1976) Ground water systems in Iceland traced by Deuterium. *Societas Scientiarum Islandica* 42:236
- Arnórsson S, Gunnlaugsson E, Svavarsson H (1983) The chemistry of geothermal waters in Iceland. III. Chemical Geothermometry in geothermal investigations. *Geochim Cosmochim Acta* 47:567–577
- Biswas SK (1987) Regional tectonic framework, structure and evolution of the western marginal basins of India. *Tectonophysics* 135:307–327
- Biswas SK (1999) A review on the evolution of rift basins in India during Gondwana with special reference to western Indian basin and their hydrocarbon prospects. *PINSA* 65A(3):216–283

- Bruhn D, Manzella A, Vuataz F, Faulds J, Moeck I, Erbas K (2011) Exploration methods. In: Huenges E (ed) geothermal energy systems. Wiley-VCH Verlag GmbH, Weinheim, p 465
- Durov SA (1948) Classification of natural waters and graphical representation of their composition. Dokl Akad Nauk USSR 59(1):87–90
- Fournier RO (1977) Chemical geothermometers and mixing models for geothermal systems. *Geothermics* 5:41–50
- Fournier RO (1979) A revised equation for the Na/K geothermometer. *Geotherm Resour Counc Trans* 3:221–224
- Fournier RO, Potter RW (1982) A revised and expanded silica (Quartz) Geothermometer. *Geotherm Resour Counc Bull* 11:3–12
- Fournier RO, Truesdell AH (1973) An empirical Na–K–Ca geothermometer for natural waters. *Geochim Cosmochim Acta* 37(5):1255–1275
- Geological Survey of India (GSI) (1991) Geothermal atlas of India, pp 1–144
- Giggenbach WF (1986) Graphical techniques for the evaluation of Water/Rock equilibration conditions by use of Na, K, Mg, and Ca-contents of discharge waters. In: Proceedings, the 8th New Zealand geothermal workshop
- Giggenbach WF (1988) Geothermal solute equilibria, derivation of the Na–K–Mg–Ca geothermometers. *Geochim Cosmochim Acta* 52:2749–2765
- Giggenbach WF (1991a) Chemical techniques in geothermal exploration. In: D'Amore F (ed) Applications of geochemistry in geothermal reservoir development. UNITAR/UNDP publication, Rome, pp 119–142
- Giggenbach WF (1991b) In: Kharaka, Maest (eds) The composition of gases in geothermal and volcanic systems as a function of tectonic setting in water–rock interactions. Balkema, Rotterdam, pp 873–878
- Giggenbach WF, Goguel RL (1989) Collection and analysis of geothermal and volcanic water and gas discharges. DSIR report CD 2401, 4th ed., Pentone
- Kiryukhin A, Xu T, Pruess K, Apps J, Slotvsov I (2003) Rastog Thermal–hydrodynamic–chemical (THC) modeling based on geothermal field data. *Geothermics* 33:349–381. <https://doi.org/10.1016/j.geothermics.2003.09.005>
- Kothiyari GC, Rastogi BK (2013) Tectonic control on drainage network evolution in the upper Narmada valley: implication to neotectonics. *Hindawi Publ Corp Geogr J* 2013:1–9
- Kumar P, Yuan X, Kumar MR, Kind R, Li X, Chadha RK (2007) The rapid drift of the Indian tectonic plate. *Nature* 449:895–897
- Lajwe G (2013) Comparison, characterization, and interpretation of geothermal fluid geochemistry in the sedimentary environments of Kibiro, Panyimur, and Öxarfjörður. UNU geothermal training programme, Reykjavik, Iceland. Report 12
- Lloyd JA, Heathcoat JA (1985) Natural inorganic hydrochemistry in relation to groundwater: an introduction. Oxford Uni Press, New York, p 296
- Love D, Gootee B, Cook J, Mahan M, Spencer J (2014) An investigation of thermal spring throughout Arizona, isotopic and geological characterization, arizona basin and Range Province. Open File Report Arizona Geological Survey
- Mehr S (1995) Geology of Gujarat. Geological Society of India, Bangalore, pp 1–224
- Niaraq MS, Ardejani FD, Noorollahi Y, Porkhilal S (2017) Development of an updated geothermal reservoir conceptual model for NW Sabalan geothermal field, Iran. *Geotherm Energy* 5:14
- Nicholson K (1993) Geothermal fluids: chemistry and exploration techniques. Springer, Berlin, p 263
- Nieva D, Nieva R (1987) Developments in geothermal energy in Mexico–part twelve, a cationic geothermometer for prospecting of geothermal resources. *Heat Recovery Syst* 7(3):243–258
- Piper AM (1994) A graphic procedure in the geochemical interpretation of water analyses. *Am Geophys Union Trans* 25:914–928
- Powell T, Cumming W (2010) Spreadsheets for geothermal water and gas geochemistry. In: Proceedings, thirty-fifth workshop on geothermal reservoir engineering. Stanford University, California, pp 1–10
- Rao GSP, Tewari HC (2005) The seismic structure of the Saurashtra crust in northwest India and its relationship with the Reunion Plume. *Geophys J Int* 160(1):318–330
- Rao PBVS, Singh AK, Rao CK (2012) Regional conductance map of Saurashtra and surrounding regions. *Curr Sci* 103(2):187–193
- Rybach L, Muffler LJP (1981) Geothermal systems: principles and case histories. Wiley, New York
- Sahajpal S, Sircar A, Singh A, Vaidya D, Shah M, Dhale S (2015) Geothermal exploration in Gujarat: case study from Unai. *Int J Latest Technol Eng Manag Appl Sci* 4(5):38–47
- Sakram G, Sundaraiah R, Vishnu B, Praveen RS (2013) The impact of agricultural activity on the chemical quality of groundwater, Karanjavagu watershed, Medak district, Andhra Pradesh. *Int J Adv Sci Tech Res* 3(6):769–786
- Schoeller H (1961) Hydrodynamique dans lekarst (Ecoulement et emmagasinement). *Actes Colloques Dubrovnik* I:3–20
- Shah M, Sircar A, Vaidya D, Sahajpal S, Chaudhary A, Dhale S (2015) Overview of geothermal surface exploration methods. *Int J Adv Res Innov Ideas Educ* 1(4):55–64
- Shah M, Sircar A, Sahajpal S, Sarkar P, Sharma D, Garg S, Mishra T, Shukla Y (2017) Geochemical analysis for understanding prospectivity of low enthalpy geothermal reservoirs of Dholera. In: Proceedings, 42nd workshop on geothermal reservoir engineering, Stanford University, Stanford, pp 1–16
- Shah M, Sircar A, Shaikh N, Patel K, Thakar V, Sharma D, Sarkar P, Vaidya D (2018a) Groundwater analysis of Dholera geothermal field, Gujarat, India for suitable applications. *Groundw Sustain Dev* 7:143–176
- Shah M, Vaidya D, Sircar A (2018b) Using Monte Carlo simulation to estimate geothermal resource in Dholera geothermal field, Gujarat, India. *Multiscale Multidiscip Model Exp Des*. <https://doi.org/10.1007/s41939-018-0008-x>
- Sharma N (2013) Physico-chemical characterization of the thermal spring waters occurring in Gujarat, India, CEGE report, pp 1–16
- Singh HK, Chandrasekharam D, Trupti G, Singh B (2014) Geochemical investigations on thermal and cold springs at Dumka District, Jharkhand, India. *Int J Earth Sci Eng* 7(1):190–194
- Singh HK, Chandrasekharam D, Trupti G, Singh B (2015) Geochemical characteristic of Bakreshwar and Tantoli geothermal province, India, In: Proceedings world geothermal congress, 2015, pp 1–5
- Singh HK, Thankappan A, Mohite P, Sinha SK, Chandrasekharam D (2018) Geothermal energy potential of Tulsishyam thermal springs of Gujarat, India. *Arab J Geosci* 11:137. <https://doi.org/10.1007/s12517-018-3501-y>
- Sircar A, Shah M, Sahajpal S, Vaidya D, Dhale S, Choudhary A (2015) Geothermal exploration in Gujarat: case study from Dholera, India. *Geotherm Energy* 3:22
- Tewari HC, Rao GSP, Prasad BR (2009) Uplifted crust in parts of western India. *J Geol Soc India* 73:479–488
- Todd DK (1980) Groundwater hydrology. Wiley, New York
- Truesdell AH, Hulston JR (1980) Isotopic evidence on environments of geothermal systems. In: Fritz P, Fontes JCh (eds) Handbook of environmental isotope geochemistry, 1, The terrestrial environment. Elsevier, Amsterdam, pp 179–226
- Urzua L, Powell T, Cumming W, Dobson P (2002) Apacheta a new geothermal prospect in northern Chile. In Geothermal resources council annual meeting transactions, p 26

- Vaidya D, Shah M, Sircar A, Sahajpal S, Dhale S (2015) Geothermal energy: exploration efforts in India. *Int J Latest Res Sci Technol* 4(4):1–23
- WHO (2004) Guidelines for drinking water quality, recommendations, vol 1, 3rd edn. WHO, Geneva, pp 1–515
- Wishart DN (2015) Comparison of silica and cation geothermometers of bath hot springs. Jamaica WI. In: Proceedings world geothermal congress, Melbourne, pp 1–13
- Zimik HV, Farooq SH, Prusty P (2017) Geochemical evaluation of thermal springs in Odisha, India. *Environ Earth Sci* 76:593